Density distribution reconstruction of the detonation front of high explosives using synchrotron radiation data

K.A. Ten[a,*], O.V. Evdokov[c], I.L. Zhogin[c], V.V. Zhulanov[b], P.I. Zubkov[a], G.N. Kulipanov[b], L.A. Luk'yanchikov[a], L.A. Merzhievsky[a], B.Ya. Pirogov[c], E.R. Pruuel[a], V.M. Titov[a], B.P. Tolochko[c], M.A. Sheromov[b]

[a]*Lavrentiev Institute of Hydrodynamics, 630090, Novosibirsk, Russian Federation*
[b]*Budker Institute of Nuclear Physics, 630090, Novosibirsk, Russian Federation*
[c]*Institute of Solid State Chemistry and Mechanochemistry, 630128, Novosibirsk, Russian Federation*

Available online 14 March 2005

Abstract

This work suggests and realizes a new method applying synchrotron radiation for remote measurement of density distribution at the front of a detonation wave. X-radiation was registered by a one-dimension gas detector DIMEX with a resolution of $100 \, \mu m$. The experimental setup is described. The methods for density reconstruction by measured intensity of transmitted radiation are also presented.
© 2005 Elsevier B.V. All rights reserved.

PACS: 07.85.F; 47.40.N; 78.70.D; 82.40.P

Keywords: High explosive; Detonation; Density; X-ray; Synchrotron radiation

1. Introduction

The classical detonation theory implies that there is a shock jump followed by the zone of chemical reaction, where pressure falls down and the substance expands up to the Chapman–Jouguet parameters. There is a few information on the processes in the reaction zone first of all because its dimensions are small ($< 1 \, mm$), the determining processes run with high rates ($\sim 0.1 \, \mu s$) and the medium is ultimately aggressive. At the same time, processes that run in this zone (high-temperature and high-pressure conversions, phase transformations, etc) cannot be realized in any other conditions. The existing methods to measure substance parameters in the chemical reaction zone either perturb the process to be measured (pressure transducers) or use an intermediate substance (foil or bromoform). The velocity of explosive charge end motion is measured most

---

*Corresponding author. Tel.: +3832 33 19 11; fax: +3832 33 16 12.

E-mail address: ten@hydro.nsc.ru (K.A. Ten).

accurately with the help of the laser methods. The only non-perturbing experimental way to measure substance parameters (density included) at a distance is now the X-ray diagnostics with SR application [1,2].

2. Experimental set-up

We used powdered RDX, HMX, PETN and TNT. Before the experiment, all the high explosives were re-crystallized with the help of acetone. The diameter of the explosive charges was 10–19.5 mm and their length was 8–10 calibres. The charges were initiated by a high-voltage detonator and a powdered octogen primer. Charges of more than 12.5 mm in diameter were initiated by an explosive lens. The experiments were carried out at the station for explosion process study at channel "0" of the VEPP-3 storage ring at Budker Institute of Nuclear Physics SB RAS. The explosive charge (E) was placed horizontally (Fig. 1) along the shaped SR beam of the following dimensions: 0.4 mm in height and 18 mm in width. The SR beam plane was passing along the axis of the explosive charge under study. The detonation front (D) took positions 1, 2 and 3 sequentially, staying in the SR beam zone for
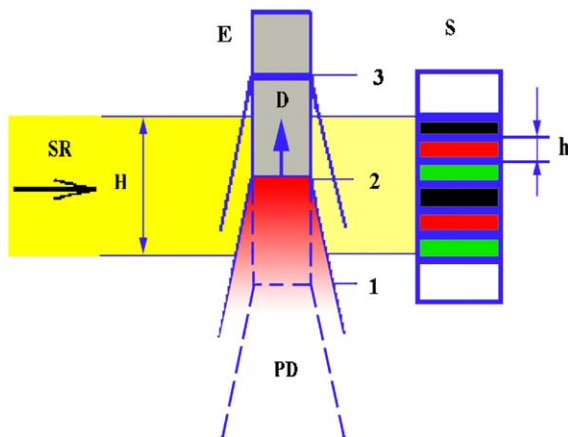

Fig. 1. Scheme of the experimental setup. E is the explosive charge, SR the SR beam plane, H the beam width, S the DIMEX detector, h the registration channel width, D the detonation front position at time instants 1, 2 and 3 and PD is the scattering products of detonation.

3–4 μs. We managed to take 3–5 momentary shots (with an exposition time of 1 ns) of the radiation passing along the charge axis in that time. The time between adjacent frames was determined by the time of electron beam rotation in the accelerator and was 250 or 500 ns. The radiation was being registered by the DIMEX detector (S), which was also situated along the charge axis at a distance of 770 mm from the object E. One registration channel was 1 mm in height and 0.1 mm along the charge axis. The total number of channels was 256 (25.6 mm). The detector was initiated via closure of a contact sensor installed at 15 mm behind the zone of view.

3. Gas detector DIMEX

Operation of the high-speed X-ray detector DIMEX is described in detail in Ref. [3]. In order to decrease the influence of the volume charge of ions in the working gas, as well as to eliminate distortions due to irradiation of the detector by an intense beam during reading of information, the time of irradiation of the detector was reduced significantly. We installed a high-speed gate (a rotating copper disk with a slit) upstream of the detector. That gate provided exposure of the detector only while the detonation front was passing, for ≈ 40 μs. Introduction of such a high-speed gate as well as a change of the detector geometry resulted in the increase of the dynamical range by a factor more than 4. The modified characteristics of the DIMEX time resolution is better than 100 ns. Fig. 2 shows the SR beam profile cut by the slit. The abscissa is the detector registration channel number; the ordinate is the registered signal value in ADC readings. The spatial resolution (FWHM) is ≈ 190 μm and determine the instrumental broadening (or instrumental function). The number of frames is 32.

4. Test experiments correction of the signal measured

The test experiments were carried out with PMMA (polymethylmethacrylate) samples. A cylinder of
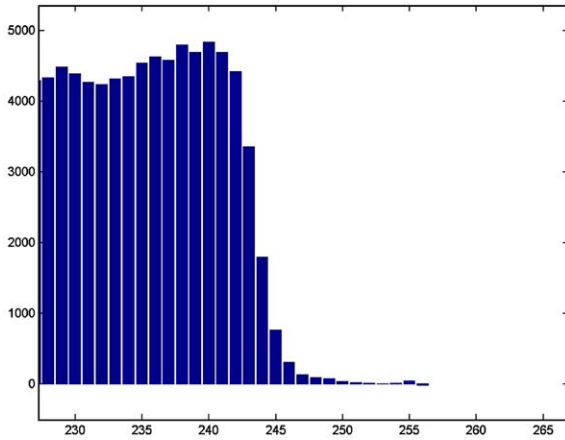
Fig. 2. Spatial resolution of the detector DIMEX. The knife closes the radiation to the right from channel 243. The abscissa is the detector registration channel number; the ordinate is the registered signal value in ADC readings.
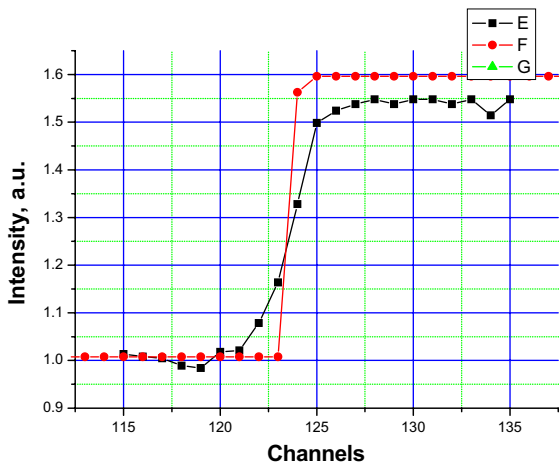

Fig. 3. Detector dates (E) vs. the channel number at irradiation of the solid cylinder. The corrected detector dates (F).

8.4 mm in diameter was installed vertically (normally to the beam plane). Fig. 3 shows distribution of the transmitted radiation intensity on the right border (E, the Y-axis) as a function of the radius (the channel number by the X-axis). It is seen that detector dates are smeared in the boundaries (channel numbers 120–126). To correct detector dates in the zone of large density gradients, a computational code was created. The "instrument function" was determined by the data on the

spatial resolution of the detector (Fig. 2). Fig. 3 shows the curve F, which corresponds to a correct distribution of the transmitted radiation.

5. Results of the experiments

Fig. 4 shows three frames of the relative intensity variation (the measured intensity divided by the initial one) along the charge axis at detonation of pressed TNT. The detonation spreads towards lower detector channel numbers. The time between the first (B) and third (D) frames is 1 μs. The detonation velocity determined by the front move was $D = 7.2$ km/s. The charge diameter was 12.5 mm, its length was 100 mm. The area under study was at 10 mm from the charge end. Fig. 5 shows the relative absorption value averaged over the three experiments (H) and corrected (G) with the help of the earlier-determined "instrumental function".

6. Density reconstruction

During detonation of high explosives and subsequent expansion of explosion products, substance density varies strongly along the SR beam. Therefore, so does the absorption spectrum. Absorption by the detector DIMEX was calibrated for hexogen and other high explosives, in
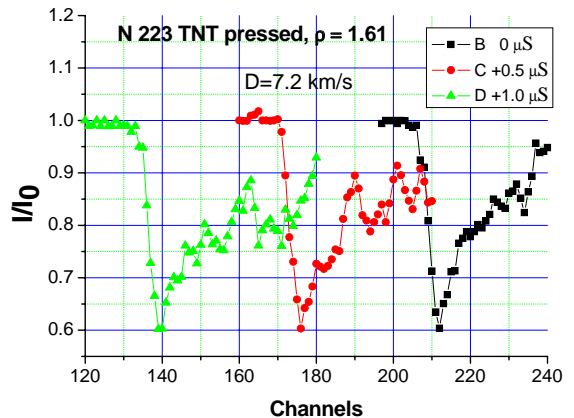

Fig. 4. Relative intensity variation along the charge axis at detonation of pressed TNT.
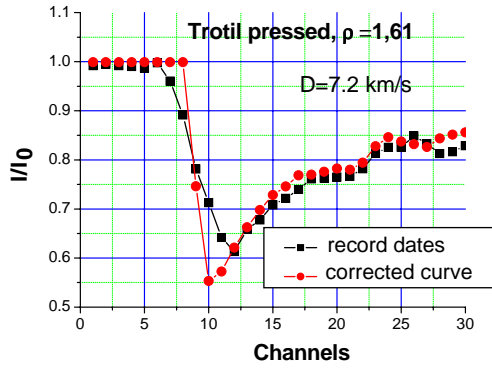
Fig. 5. Averaged and corrected intensity variation at the front along the charge axis at detonation of pressed TNT.
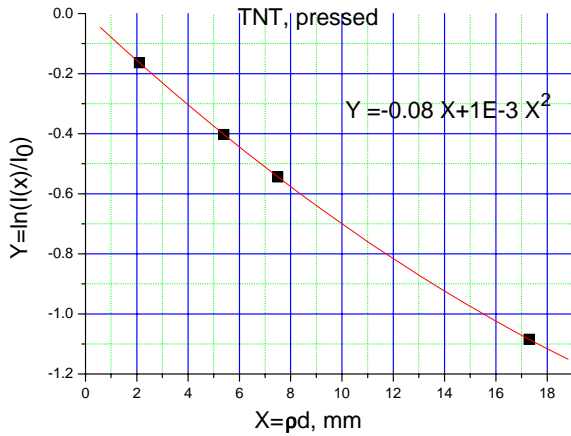

Fig. 6. Dependence of the relative TNT absorption on the $Y = \rho d$ value.

Fig. 7. Relative density variation at the front along the charge axis at detonation of powdered and pressed TNT.

dependence on the density multiplied by the charge thickness ($Y = \rho d \, \mathrm{g/cm^2}$). All the channels were calibrated simultaneously. The relative absorption logarithm for one channel is presented in Fig. 6. The curve can be interpolated well with a parabola, the coefficient of Y^2 being less more than an order than that of Y.

Absorption before the experiment can be written in the following form:

$$J_{\text{before}} = J_{\text{air}} \exp(-\beta_2 \rho_0 d)$$
$$= J_{\text{air}} \exp(-\alpha_1 \rho_0 d + \alpha_2(\rho_0 d)^2),$$

where J_{air} is the initial SR flux, β_2 the absorption coefficient for this charge, α_1 and α_2 the interpolated ab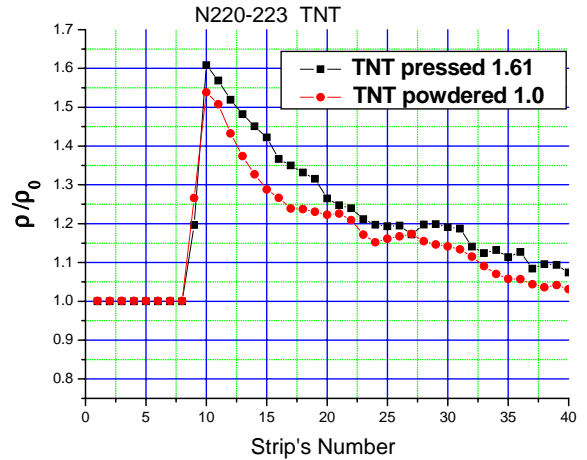sorption coefficient (see Fig. 7), ρ_0 the initial density and d is the charge diameter. The intensity recorded by the detector can be written in the following form:

$$J_{\text{exp}} = J_{\text{air}} \exp(-\alpha_1 \rho_x d + \alpha_2(\rho_x d)^2).$$

Then, the records in Fig. 5 can be presented as follows:

$$\frac{J_{\text{exp}}}{J_{\text{before}}} = \frac{\exp(-\alpha_1 \rho_x d + \alpha_2(\rho_x d)^2)}{\exp(-\alpha_1 \rho_0 d + \alpha_2(\rho_0 d)^2)},$$

where ρ_x is the desired density. It is implied in this formula that the charge diameter is not changing. That is, density is determined at the wave front only or at time moments when product spread can be neglected.

The value $\frac{J_{\text{before}}}{J_{\text{air}}}$ was also recorded in each of the experiments,

$$\ln\left(\frac{J_{\text{exp}}}{J_{\text{before}}}\right) = -\alpha_1(\rho_x - \rho_0)d + \alpha_2(\rho_x^2 - \rho_0^2)d^2,$$

$$\ln\left(\frac{J_{\text{before}}}{J_{\text{air}}}\right) = -\alpha_1 \rho_0 d + \alpha_2 \rho_0^2 d^2 = -\beta_2 \rho_0 d.$$

Then the ratio of the logarithms $\frac{J_{\text{exp}}}{J_{\text{before}}}$ and $\frac{J_{\text{before}}}{J_{\text{air}}}$ equals

$$g = \frac{\ln(J_{\text{exp}}/J_{\text{before}})}{\ln(J_{\text{before}}/J_{\text{air}})} = \frac{-\alpha_1(\rho_x - \rho_0)d + \alpha_2(\rho_x^2 - \rho_0^2)d^2}{-\beta_2 \rho_0 d}$$

$$= \frac{\alpha_1}{\beta_2}\left(\frac{\rho_x}{\rho_0} - 1\right) - \frac{\alpha_2}{\beta_2}\rho_0 d\left(\left(\frac{\rho_x}{\rho_0}\right)^2 - 1\right).$$

One can derive a quadratic equation for $\frac{\rho_x}{\rho_0}$,

$$\left(\frac{\rho_x}{\rho_0}\right)^2 - \left(\frac{\rho_x}{\rho_0}\right)\frac{\alpha_1}{\alpha_2\rho_0 d} + \frac{\beta_2}{\alpha_2\rho_0 d}\left(g + \frac{\alpha_1}{\beta_2}\right) - 1 = 0.$$

Its solution gives us the relative density increase at the front,

$$\left(\frac{\rho_x}{\rho_0}\right) = \frac{\alpha_1}{2\alpha_2\rho_0 d}$$
$$\pm \sqrt{\left(\frac{\alpha_1}{2\alpha_2\rho_0 d}\right)^2 - \frac{\beta_2}{\alpha_2\rho_0 d}\left(g + \frac{\alpha_1}{\beta_2}\right) + 1}.$$

The obtained density profile is presented in Fig. 7.

For the sake of comparison, the density profile was calculated by a simpler formula that does not take into account spectrum variation when ρd changes.

The ρ_x/ρ_0 values calculated by this formula are less by 4.9% than the above values. Such a small difference seems to be linked with a filter (1 mm of Al) applied ahead of the charge, which cuts out the "soft" part of the spectrum.

7. Accuracy of the methods

The density determination accuracy is formed by the linear density spread ΔY due to the error in determination of α and β, detector reading error ΔJ and error $\Delta\rho$ due to uncertainty of the real diameter d and influence from the detonation front curvature. The detector reading error ΔJ at averaging over the three experiments can be considered $\approx 1\%$ [3]. Then the error ΔY is determined as

$$\left|\frac{\Delta Y}{Y}\right| = \approx 0.8\% + 1.0\% = 1.8\%.$$

Analyzing the detector records and shots of the high-speed photo-recorder, one can see that smearing of boundaries is less than 0.15 mm. The front curvature (its maximal convexity) is not registered in the shots and by the detector. It is estimated to be less than 0.15 mm.

Thus, in this experimental setup, the density determination error in the first detector channels

(at the detonation front) is

$$\frac{\Delta\rho}{\rho} = \left|\frac{\Delta Y}{Y}\right| + \left|\frac{\Delta d}{d}\right| \approx 1.8\% + 1.2\% = 3.0\%.$$

Detector dates in the subsequent channels give the average density along the SR beam.

Let us estimate the influence of the sideways scatter of the explosion products. The sound speed in the detonation products behind the front is $C \approx 5\,\text{km/s}$. At a distance of 1 mm, the smearing zone of the sideways scatter is $\Delta X \approx \frac{5}{7.3} = 0.68\,\text{mm}$.

The initial diameter being 12.5 mm, the density determination error is $\sim 5.4\%$.

8. Conclusion

These experimental data on density at the detonation wave front in hexogen are in good agreement with those in literature [4], which were obtained in other experimental setups. The obtained spatial resolution of $\sim 150\,\mu\text{m}$ makes it possible to study transient processes at initiation of detonation as well as substance parameters at the shock wave front. At the moment, these methods resolution is limited by the spatial resolution of the X-ray detector.

References

[1] A.N. Aleshaev, P.I. Zubkov, G.N. Kulipanov, L.A. Luk'yanchikov, N.Z. Lyakhov, S.I. Mishnev, K.A. Ten, V.M. Titov, B.P. Tolochko, M.G. Fedotov, M.A. Sheromov, Phys. Combust. Explos. 37 (5) (2001) 104 (in Russian).
[2] A.N. Aleshaev, A.M. Batrakov, M.G. Fedotov, G.N. Kulipanov, N.Z. Lyakhov, L.A. Luk'yanchikov, S.I. Misnev, M.A. Sheromov, K.A. Ten, V.M. Titov, B.P. Tolochko, P.I. Zubkov, Nucl. Instr. and Meth. A 470 (1–2) (2001) 240.
[3] V. Aulchenko, Evdokov, S. Ponomarev, L. Shekhtman, K. Ten, B. Tolochko, I. Zhogin, V. Zhulanov, Nucl. Instr. and Meth. A 513 (1–2) (2003) 383.
[4] A.N. Dremin, S.D. Savrov, V.S. Trofimov, K.K. Shvedov, Detonation waves in condensed media, Science (Moscow) (1970) 164 (in Russian).